MEASUREMENT OF THE DIFFRACTIVE REACTION

$\pi^- p \to \pi^- \pi^- \pi^+ p$ AT 93 GeV/c

B. Alper, H. Becker, I. Blakey, G. Blanar, W. Blum, M. Bowler,
R. Cashmore, M. Cerrada, V. Chabaud, C. Damerell, C. Daum, J. De Groot,
H. Dietl, A. Dwurazny, J. Gallivan, A. Gillman, M. Glaubman, C. Hardwic
L. Hertzberger, W. Hoogland, M. Hotchkiss, B. Hyams, R. Jongerius,
R. Klanner, J. Loken, E. Lorenz, G. Lütjens, G. Lutz, W. Männer,
S. Peters, G. Polok, R. Richter, M. Rozanska, K. Rybicki, J. Spalding.
U. Stierlin, G. Thompson, H. Tiecke, M. Turala, J. Turnau,
P. Van Deurzen, P. Weilhammer and F. Wickens.

Amsterdam-CERN-Cracow-Munich-Oxford-Rutherford Collaboration

ABSTRACT

Data are presented from a measurement of the diffractive reaction $\pi^- p \to \pi^- \pi^- \pi^+ p$ at a beam momentum of 93 GeV. The experiment was performed with a modular two-magnet forward spectrometer at the CERN SPS and yielded almost one quarter of a million events.

The differential cross-section shows clear evidence of a two-component structure for all 3π masses below 2 GeV/c^2, a phenomenon not previously observed in diffractive dissociative reactions.

Preliminary results from a partial wave analysis show the 1^+S intensity at low and high momentum transfer. The $2^+D_{M=1}$ (A_2) Breit-Wigner is extracted and mass and width parameters presented with, in addition, the differential cross-section and polarization. In the high mass region the intensity of the 2^-S (A_3) wave is presented and the cross-sections of all three major contributing terms are compared as a function of beam momentum.

Submitted to the XIX Int. Conf. on High Energy Physics, Tokyo 1978

1. THE APPARATUS

The data presented here are from an experiment carried out at CERN using an unseparated hadron beam from the SPS.

The apparatus consisted of a liquid hydrogen target, a 2 magnet forward spectrometer equipped with 2 large aperture Cerenkov hodoscopes and wire spark chambers. (See fig.1 of [1] for a schematic plan of the spectrometer).

The 2 magnet configuration permitted the measurement of both low and high momentum secondaries with good acceptance.

Scintillator and proportional chamber hodoscopes were used to select the forward charged multiplicity. Multiprong events, as for example from target fragmentation, were vetoed by counter arrays around the target and before the first magnet.

Data from the reaction

$$\pi^- p \to \pi^- \pi^- \pi^+ p \qquad (1)$$

were taken at 93.7 GeV/c, the highest useful momentum available from the beam. From a total of $8.3 \cdot 10^5$ triggers, $2.1 \cdot 10^5$ events remained after applying vertex cuts, Cerenkov identification requirements and cuts to the missing mass of the unmeasured recoil system. A multineutral background of $2 \pm 1\%$ remains.

2. THE DATA

The (3π) mass spectrum from reaction (1) is shown in fig.1 together with the data corrected for acceptance. A large part of this correction is due to unbiased losses from veto counters. The spectrum is similar to that obtained by experiments of lower energy and smaller statistics though there is now the possibility of structure in the flat top of the 1.1 to 1.3 GeV/c^2 "A_1" region.

The differential cross-section $d\sigma/dt'$ in the region below a three pion mass of 2 GeV/c^2 is, however, considerably different from previous observations which have either been in limited ranges of momentum transfer ($t' = t - t_{min}$ is used throughout this paper) or of too small statistics. The usual mass-dependence of the slope is observed at low $|t'|$ but there

is a clear break in slope in the region of 0.4 $(GeV/c)^2$, this second component having a smaller and non-mass-dependent slope of about $5(GeV/c)^{-2}$. This break in slope is best observed at low masses, as for example in fig.2. Various parametrizations have been attempted to describe this phenomenon up to cubic expressions in a single exponential, and also involving additions of terms disappearing in the forward direction ($t'A\,e^{At'}$) to test the possibility that the observation was one of very large tails from the A_2. The best fit was to the simple, incoherent, two component function

$$p\,A\,e^{At'} + (1 - p)\,B\,e^{Bt'}$$

The values of the two slopes A(m), B(m) as a function of (3π) mass may be seen in fig.3 and the value of the fraction p is similarly shown in fig.4. The A_2 does have a perturbing effect, but the phenomenon is present throughout the entire (3π) mass spectrum. In addition, it should be noted that similar behaviour is also seen in preliminary diffractive $(K\pi\pi)$ data from this spectrometer.

3. PARTIAL WAVE ANALYSIS

A mass-independent partial wave analysis of the events of reaction (1) has been carried out in 20 MeV/c^2 mass bins in the two $|t'|$ intervals $0.0 < |t'| < 0.05$ $(GeV/c)^2$ (low t') and $0.05 < |t'| < 0.7$ $(GeV/c)^2$ (high t') for 3π masses below 1.6 GeV/c^2 and for the complete range $0.0 < |t'| < 0.7$ above this value. In the isobar model used, the ρ^0 and f^0 mass and width values are taken from current data table world averages, whilst the S-wave $\pi^+\pi^-$ interaction is taken from the CERN-Munich phase shift analysis [2]. In the present analysis, waves up to and including $J = 4$ have been introduced.

The analysis has proceeded using both the amplitude parametrization of the SLAC program [3] and the density matrix formalism as used at Illinois [4]. A detailed comparison of these techniques will be presented elsewhere [5] but no serious discrepancies have yet been found. This publication is based on results from density matrix fits.

The intensity of the dominant 1^+S $(\rho\pi)$ wave* of the low mass region may be seen in fig.5 at low t', where the shape is that of a steep rise

---

* The nomenclature $J^P\ell$ is used with ℓ giving the angular momentum between the isobar and the remaining pion in spectroscopic notation. Unless otherwise stated, M = 0 states are implied.

to 1.1 GeV/c^2 and slow fall-off common to many threshold-type phenomena. This changes radically at high t' as is shown in fig.6, although the leading edge and peak are still similar.

Adding these plots together and integrating between mass values of 1.0 and 1.2 GeV/c^2 gives a cross-section representative of this intensity which may be compared to other data [6] in fig.7. The rate of decrease is indeed very small and, if fitted to a functional dependence on laboratory momentum of p^{-n}, yields $n = 0.32 \pm 0.04$.

The A_2 is a well-established resonance and, as may be seen from the intensity of the $2^+D_{M=1}$ ($\rho\pi$) wave in fig.8, seems to occur on negligible background. The solid curve in this diagram is a fit to a non-relativistic Breit-Wigner with no background, and it may be noted that the fit is somewhat inadequate, being too high at low mass and vice versa. The simple angular momentum barrier factor form $(q/q_0)^{2\ell+1}$, with q the isobar momentum at fixed ρ mass, over-corrects for this symptom producing a worse fit. The best values obtained for mass, width and cross-section of the A_2 are then

$$\text{Mass} = 1319 \pm 5 \text{ MeV}/c^2$$

$$\text{Observed Width} = 134 \pm 10 \text{ MeV}/c^2$$

$$\text{Resolution Corrected Width} = 126 \pm 10 \text{ MeV}/c^2$$

$$\text{Total Cross-Section} = 20.1 \pm 3.0 \ \mu\text{b}$$

When integrated between 1.2 and 1.4, this cross-section point lies close to the p^{-n} line though lower energy data, despite the large lever arm. The exponent fitted to all data (fig.9) has the value $n = 0.46 \pm 0.04$.

The differential cross-section for the A_2 in the mass interval $1.26 < m < 1.36$ GeV/c^2 is shown in fig.10, fitted to the functional form $t'e^{At'}$. It is clear that there is the expected dip caused by the non-existence of helicity flip in the forward direction, but the data would better fit an even steeper slope than a linear dependence. The value obtained for the slope in this parametrization is $A = 7.5 \pm 0.1$ (GeV/c)$^{-2}$, which should be compared to the slope for a simple exponential fit to the 1^+S in the same mass range which gives $A = 9.4 \pm 0.1$ (GeV/c)$^{-2}$.

In the limited mass and t' range of $1.30 \leq m \leq 1.33$ GeV/c^2 and $0.02 < |t'| < 0.3$ (GeV/c)^2 all possible M states of the 2^+D wave have been included in order to derive the complete density matrix of Table I. As in the partial wave analysis, states are here arranged to be eigenvalues of the reflection parity operator such that, in the high energy limit, they correspond to natural and unnatural parity exchange states. It is clear that at this momentum, the contribution from unnatural parity exchange is zero within errors.

Table I

A_2 polarization

$1.30 \leq m < 1.33$, $0.02 \leq |t'| \leq 0.03$

"Natural Parity Exchange"	
$\rho_{11} + \rho_{1-1}$	0.95 ± 0.06
$\rho_{22} - \rho_{2-2}$	0.02 ± 0.09
Re (ρ_{21})	0.02 ± 0.06
Im (ρ_{21})	-0.05 ± 0.20
Trace	0.96 ± 0.09
"Unnatural Parity Exchange"	
Trace	0.04 ± 0.09

At high masses, statistics at present limit the analysis to only one bin of momentum transfer, $0.0 < |t'| < 0.7$. The intensity for the 2^-S ($f\pi$) wave (the A_3) is plotted for this interval in fig.11. A non relativistic Breit-Wigner with no background of rather large width may be fitted and yields the parameters:

Mass A_3 : 1647 ± 5 MeV/c

Observed Width A_3 : 306 ± 10 MeV/c

It should be noted that, at this stage, these values are quoted merely for a parametrization and are not intended to necessarily imply resonance status. If the intensity is integrated between 1.5 and 1.8 GeV/c^2 for

comparison with other experiments (fig.12) a fit to the exponent of the laboratory momentum gives n = 0.26 ± 0.07. It could be that this is compatible with the value 0.32 ± 0.04 for the 1^+S intensity, and neither of them with the value 0.46 ± 0.04 obtained for the A_2, even though this value has decreased somewhat from the figure of 0.51 ± 0.05 quoted [6] before this experiment.

4. CONCLUSIONS

The differential cross-section of a diffractive dissociative reaction has been shown to have other than a simple exponential dependence, the break in the slope being best parametrized by an incoherent two component model.

Preliminary results from a partial wave analysis have extracted a clear A_2 Breit-Wigner resonance and the full parametrization including differential cross-section has been presented. The same analysis shows that the shape of the 1^+S intensity changes as a function of momentum transfer. The cross-section for this wave falls off at a rate which is compatible with the fall off of the 2^-S (A_3) intensity, but both are somewhat smaller than the rate of decrease of the A_2 cross-section.

[4] Hansen et al., Nuclear Phys. B81 (1974) 403.
[5] W.J. Spalding. Thesis, to be published.
[6] Yu.M. Antipov et al., Nuclear Phys. B63 (1973) 153.

Figure captions

Fig. 1 : Mass spectrum of the $(3\pi)^-$ system of reaction (1) in the range $0 \leq |t'| \leq 0.5$ $(GeV/c)^2$. The solid line shows the result of acceptance corrections from all sources except losses from secondary interactions and decays which account for 15% of real events in a negligibly biased fashion.

Fig. 2 : Differential cross-section in a 50 MeV/c^2 (3π) mass bin from 0.90 to 0.95 GeV/c^2 with a fit to the function $p\,Ae^{At'} + (1-p)\,B\,e^{Bt'}$, as described in the text.

Fig. 3 : Values of the slopes A,B in the above expression as a function of 3π mass.

Fig. 4 : Values of the fraction p, in the above reaction as a function of 3π mass.

Fig. 5 : Intensity of the 1^+S $(\rho\pi)$ wave for $0 < |t'| < 0.05$ $(GeV/c)^2$.

Fig. 6 : Intensity of the 1^+S $(\rho\pi)$ wave for $0.05 < |t'| < 0.7$ $(GeV/c)^2$.

Fig. 7 : Cross-section of the 1^+S for the 3π mass interval $1.0 < m < 1.2$ GeV/c^2 as a function of momentum.

Fig. 8 : Intensity of the $2^+D_{M=1}$ $(\rho\pi)$ wave for $0.05 < |t'| < 0.7$ $(GeV/c)^2$ with a fit to a non-relativistic Breit-Wigner, with no background.

Fig. 9 : Cross-section of the $2^+D_{M=1}$ wave for the 3π mass interval $1.2 < m < 1.4$ GeV/c^2 as a function of momentum.

Fig. 10 : Differential cross-section, $d\sigma/dt'$, of the $2^+D_{M=1}$ (A_2) intensity with a fit to the form $t'e^{At'}$.

Fig. 11 : Intensity of the 2^-S $(f\pi)$ wave for $0 < |t'| < 0.7$ with a fit to a non-relativistic Breit-Wigner, with no background.

Fig. 12 : Cross-section of the 2^-S wave for the 3π mass interval $1.5 < m < 1.8$ GeV/c^2 as a function of momentum.

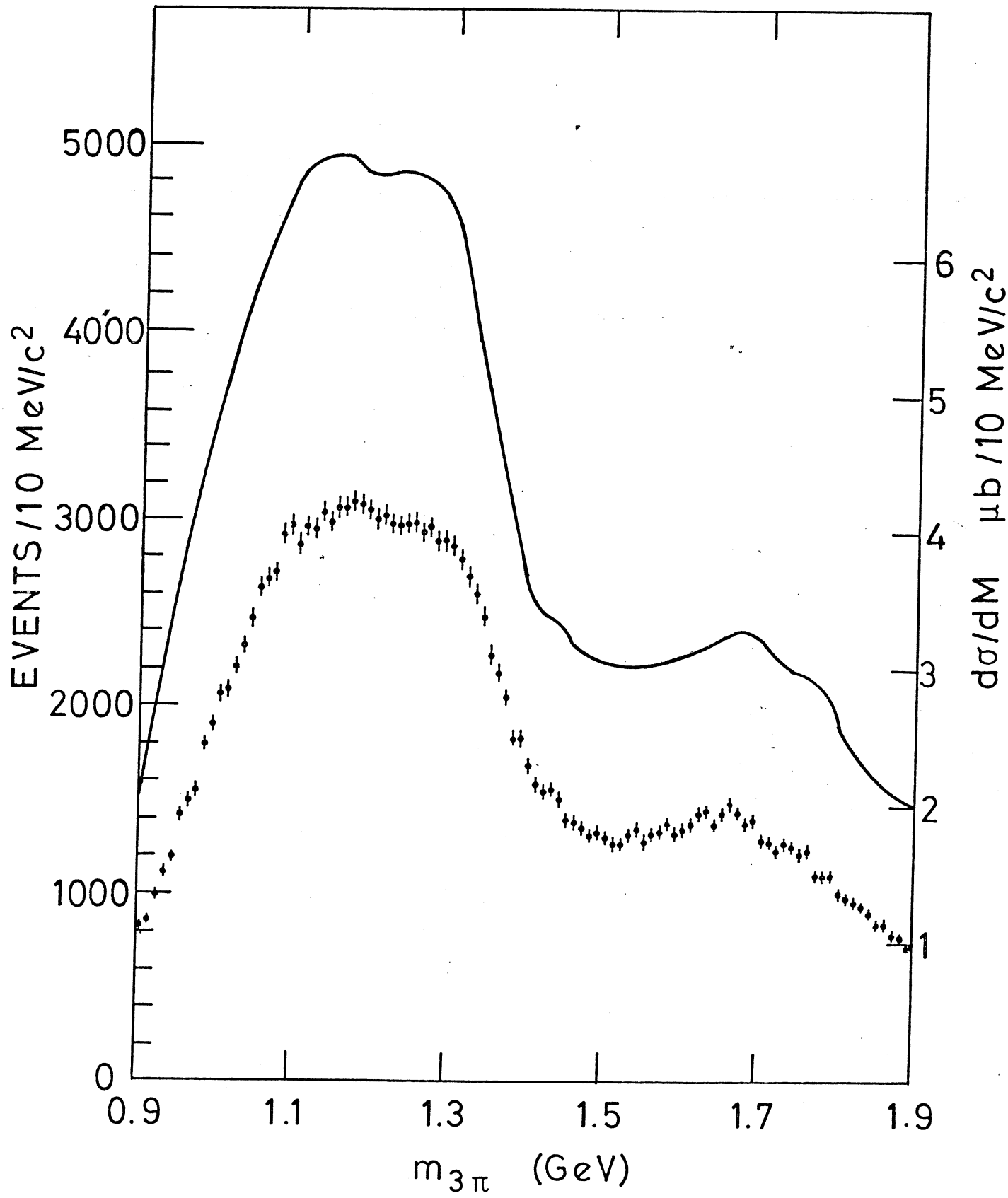
5000
4000
3000
2000
1000
0
EVENTS/10 MeV/c²
6
5
4
3
2
1
dσ/dM μb/10 MeV/c²
0.9
1.1
1.3
1.5
1.7
1.9
m3π (GeV)

Fig.1

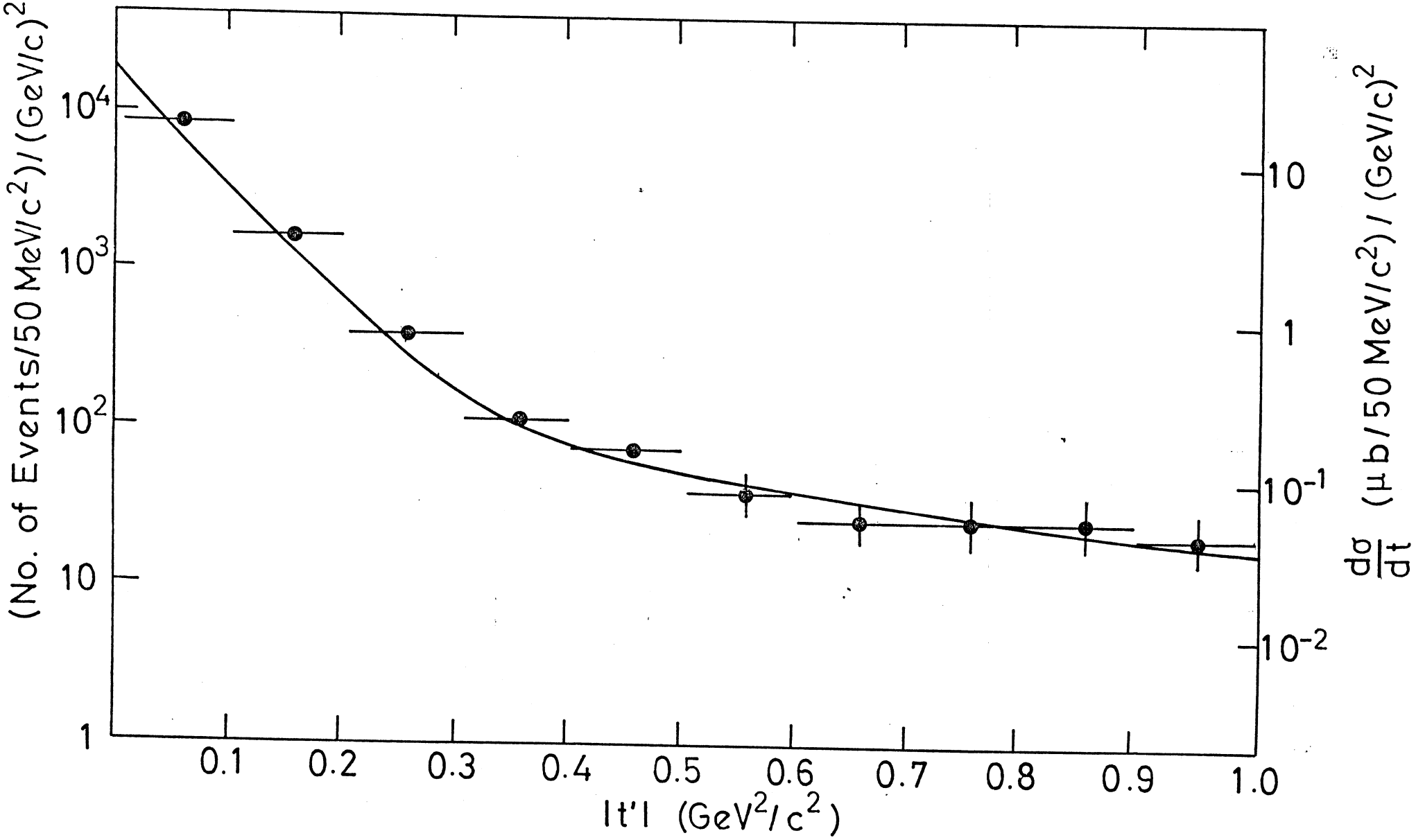
(No. of Events/50 MeV/c²)/(GeV/c)²
10⁴
10³
10²
10
1
0.1
0.2
0.3
0.4
0.5
0.6
0.7
0.8
0.9
1.0
|t'| (GeV²/c²)
10
1
10⁻¹
10⁻²
dσ/dt (μb/50 MeV/c²)/(GeV/c)²

Fig. 2

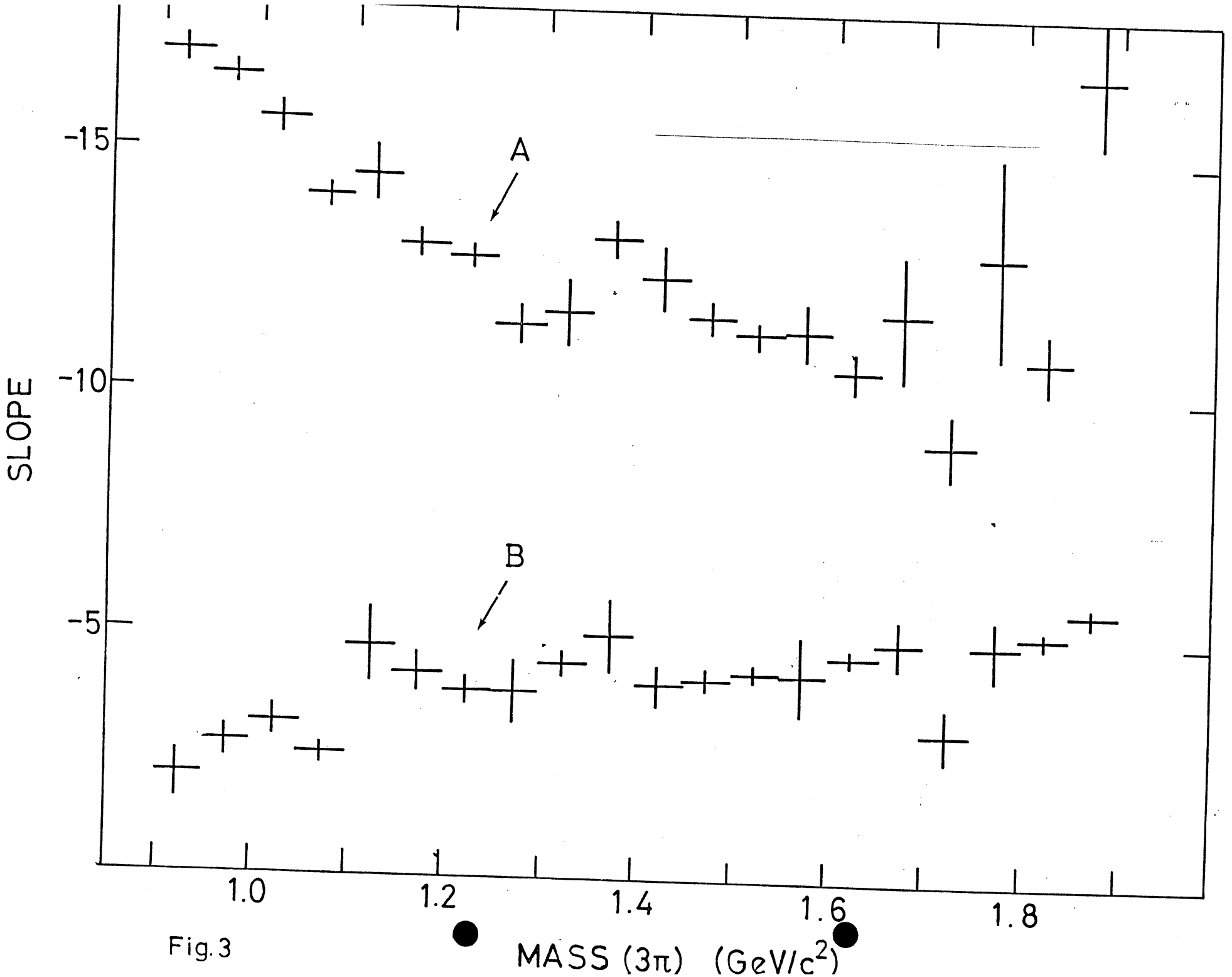

Fig. 3

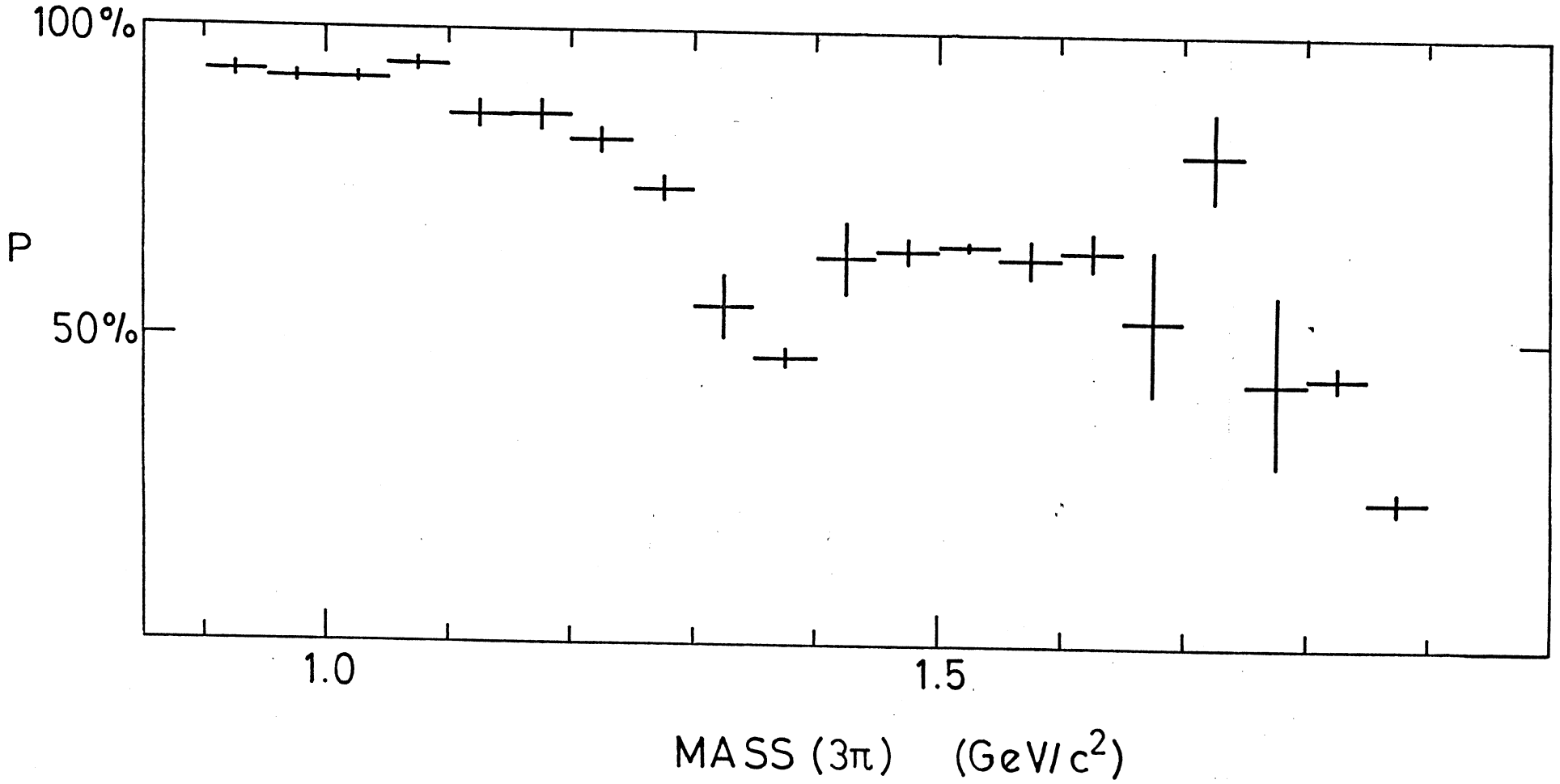

Fig. 4

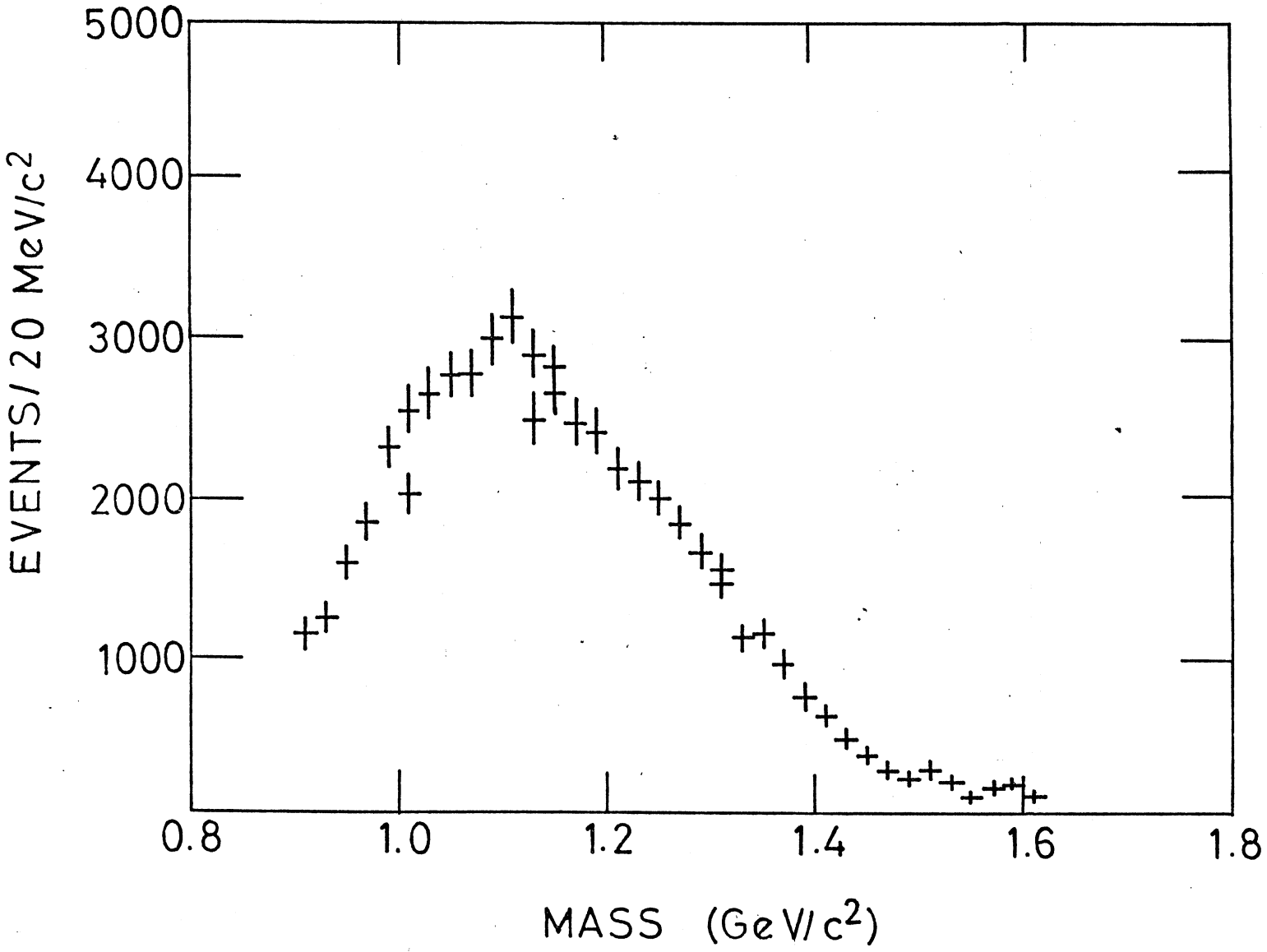
5000
4000
3000
2000
1000
EVENTS/20 MeV/c²
0.8
1.0
1.2
1.4
1.6
1.8
MASS (GeV/c²)

Fig.5

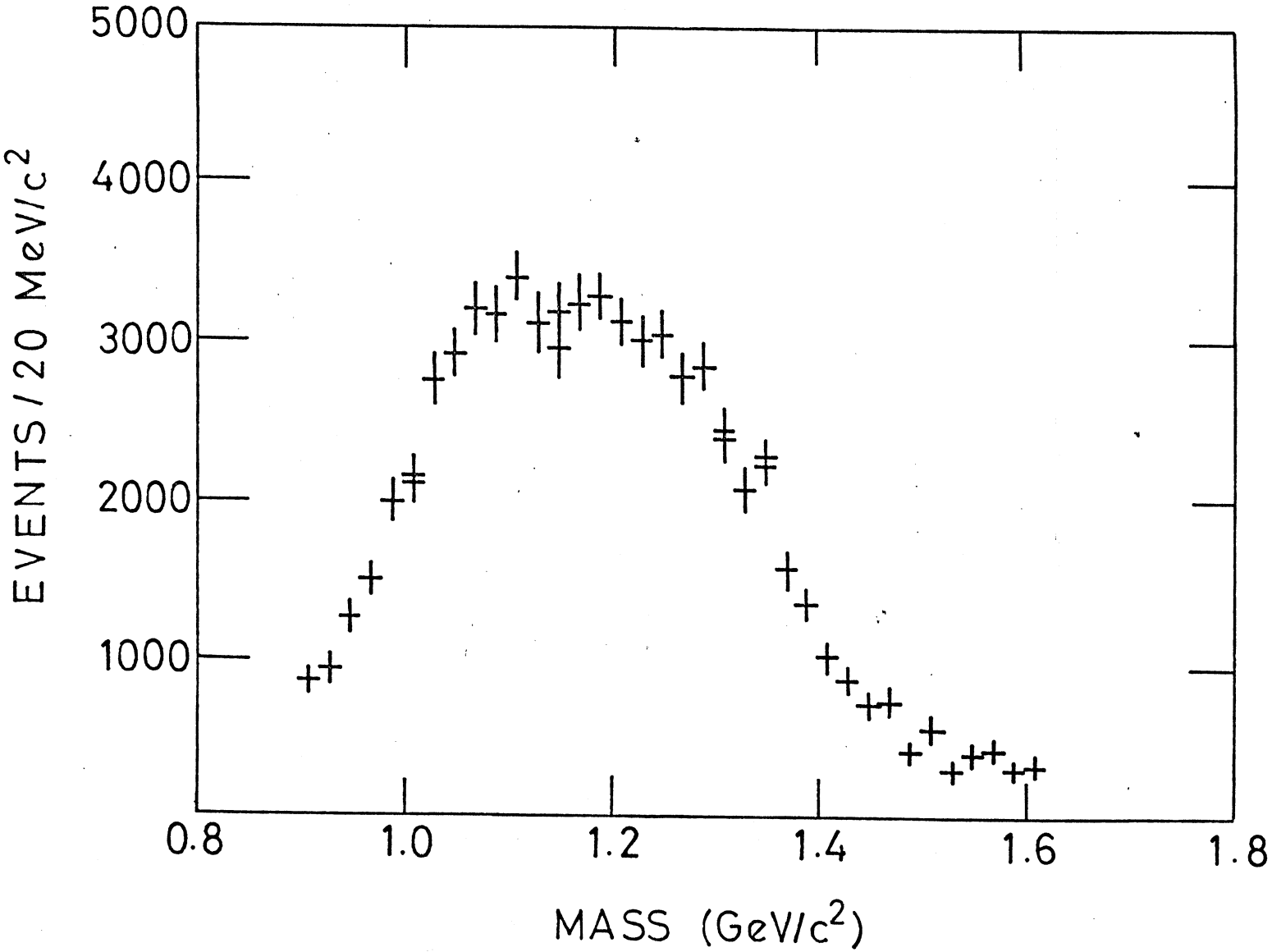
5000
4000
3000
2000
1000
EVENTS / 20 MeV/c²
0.8
1.0
1.2
1.4
1.6
1.8
MASS (GeV/c²)

Fig. 6

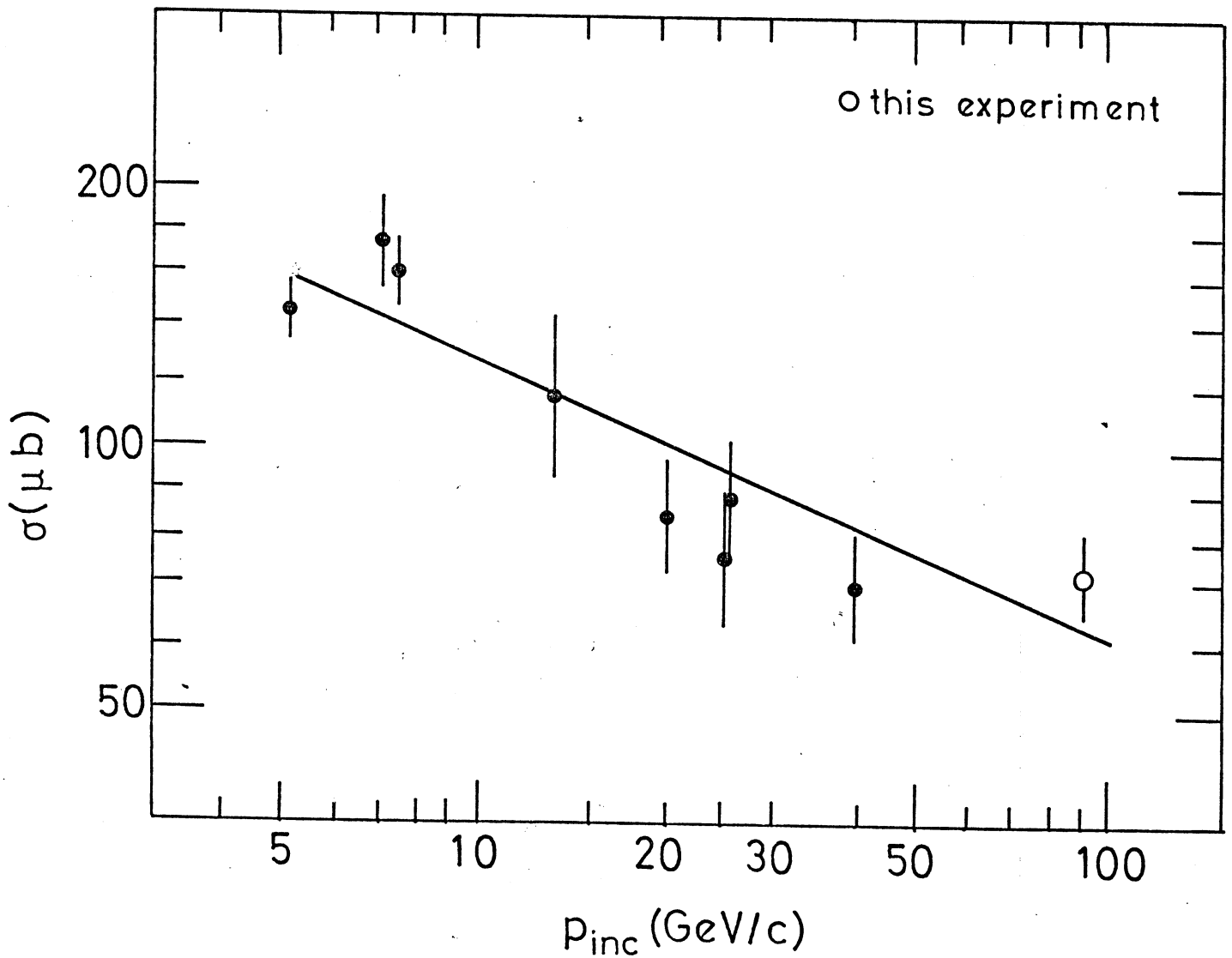

Fig. 7

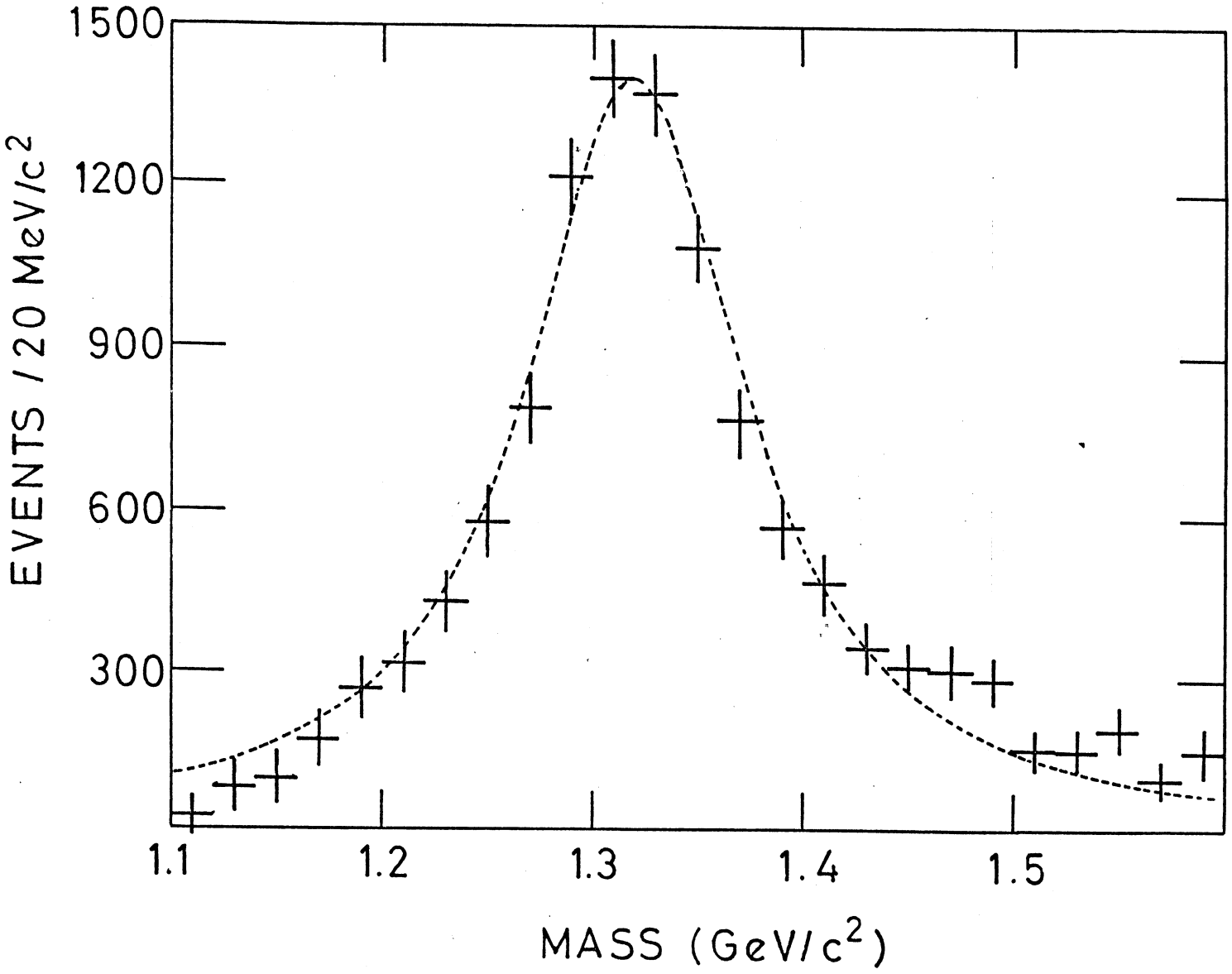

Fig. 8

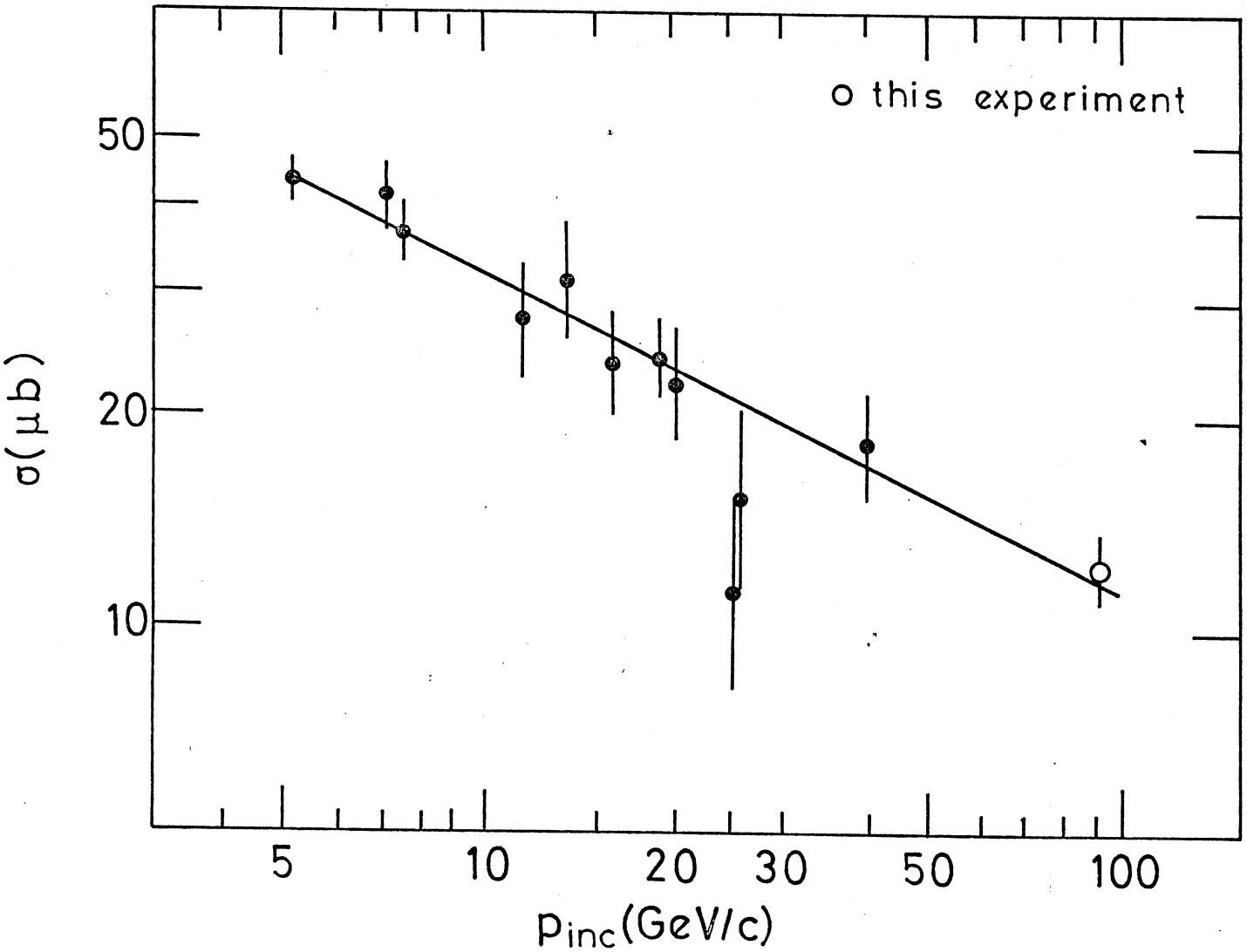

Fig. 9

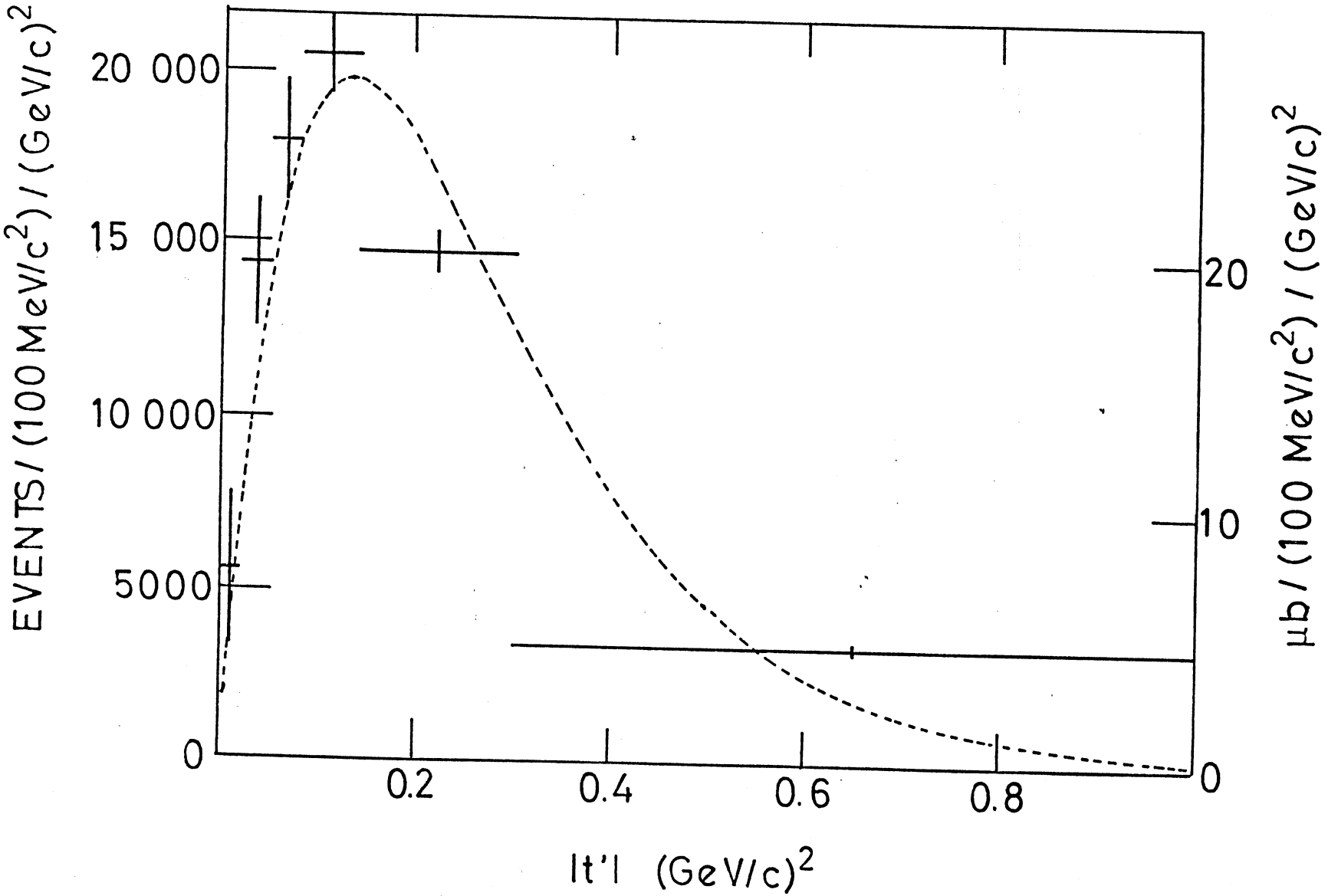
EVENTS / (100 MeV/c²) / (GeV/c)²
20 000
15 000
10 000
5000
0
0.2
0.4
0.6
0.8
|t'| (GeV/c)²
μb / (100 MeV/c²) / (GeV/c)²
20
10
0

Fig.10

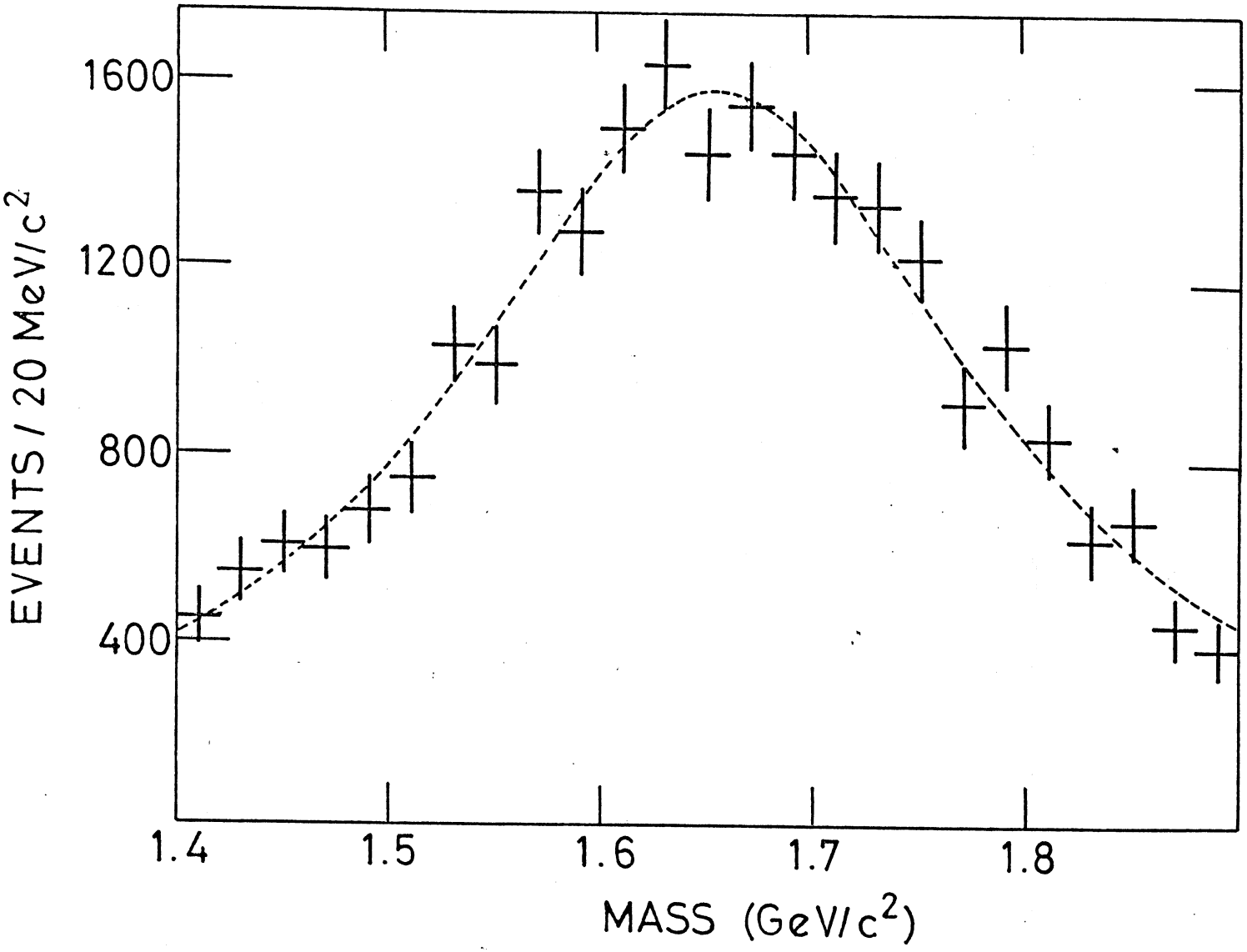

Fig. 11

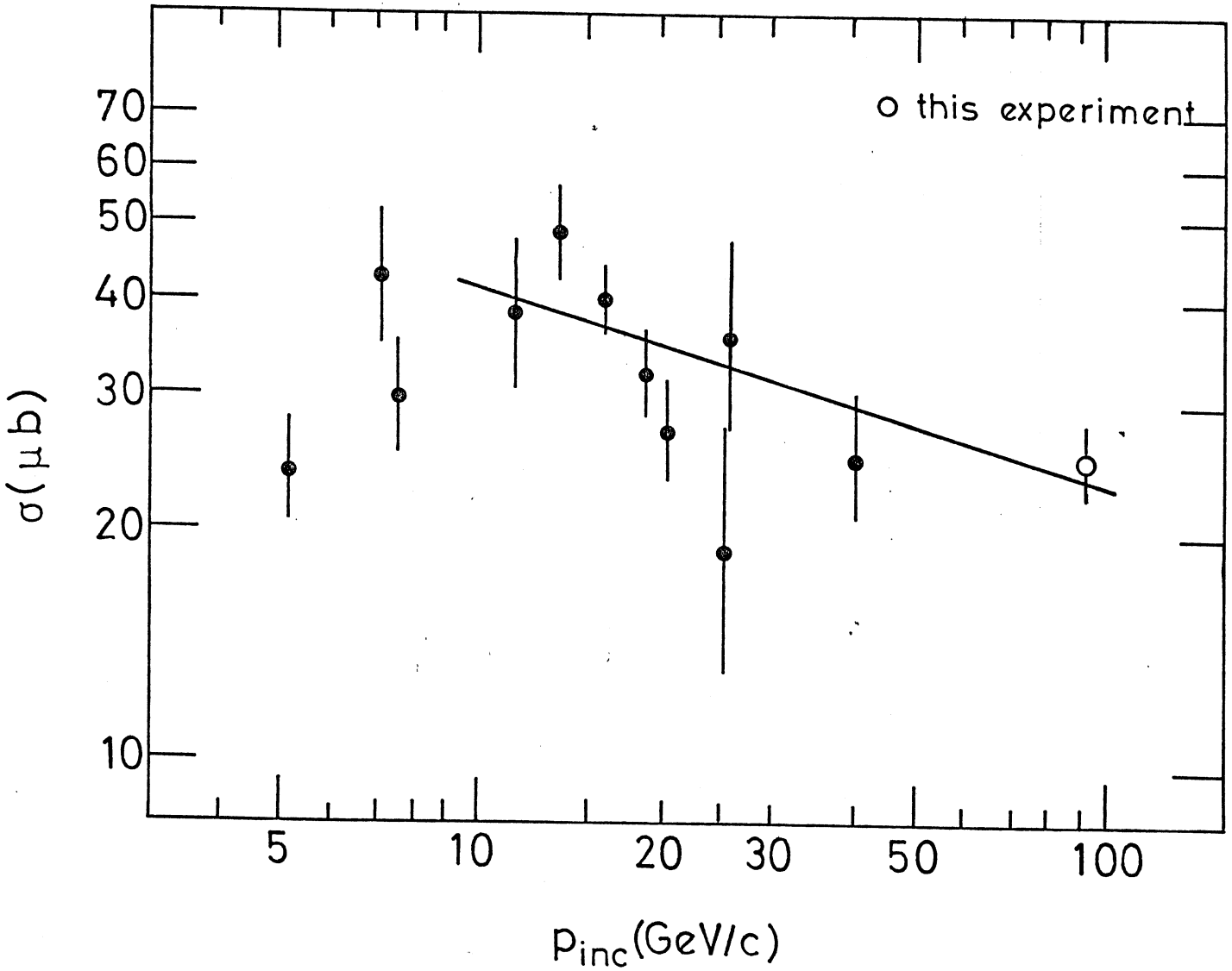
o this experiment
70
60
50
40
30
20
10
σ(μb)
5
10
20
30
50
100
p_{inc}(GeV/c)

Fig. 12